Paneth cell maturation is related to epigenetic modification during neonatal–weaning transition

Ryoko Baba (babar@med.uoeh-u.ac.jp)
University of Occupational and Environmental Health Japan
Keiji Kokubu
University of Occupational and Environmental Health Japan
Kenta Nakamura
University of Occupational and Environmental Health Japan
Mamoru Fujita
Kurume University
Hiroyuki Morimoto
University of Occupational and Environmental Health Japan

Research Article

Keywords: Paneth cells, crypts, organoids, histone modifications, epigenetic processes

Posted Date: March 10th, 2022

DOI: https://doi.org/10.21203/rs.3.rs-1429477/v1

Abstract

Paneth cells are antimicrobial peptide-secreting epithelial cells located at the bottom of the intestinal crypts of Lieberkühn. Crypts begin to form around day 7 of postnatal mice (P7), and Paneth cells usually appear within the first 2 weeks. Paneth cell dysfunction has been reported to correlate with Crohn's disease-like inflammation, showing narrow crypts or loss of crypt architecture in mice. The morphology of dysfunctional Paneth cells is similar to that of a Paneth/goblet intermediate cell. However, it remains unclear whether the formation of the crypt is related to the maturation of Paneth cells. In this study, we investigated the histological changes in the mouse ileum postnatally and assessed the effect of the methyltransferase inhibitor on epithelium development using organoid culture. The morphological and functional maturation of Paneth cells occurred in the first 2 weeks and was accompanied by histone H3 lysine 27 (H3K27) trimethylation. Inhibition of H3K27 trimethylation suppressed crypt formation and Paneth cell maturation on organoids derived from ileum of early second postnatal mouse. Overall, our data show that post-transcriptional modification of histones, particularly H3K27 trimethylation, leads to the structural and functional maturation of Paneth cells during postnatal development.

Introduction

The small intestine mucosa has an abundance of villi and crypts and, therefore, can greatly expand its surface for function. The epithelium covering the mucosal surface is renewed continuously and rapidly. The epithelium consists of absorptive cells (or enterocytes), goblet cells, enteroendocrine cells, tuft cells, and Paneth cells. All intestinal epithelial cells (IECs) originate from intestinal stem cells (ISCs) that reside in niches of the lower crypt. ISCs give rise to transient amplifying cells that become progenitor cells positioned at the bottom two-thirds of the crypts (Barker and Clevers, 2007). The activation of Notch signaling targets *Hes-1* and *Math-1* differentiates the early progenitor cells into absorptive cells and secretory cell lineages, respectively, in IECs (Fre, et al., 2005). Furthermore, in secretory cell lineages, Gfi1 functions to select goblet/Paneth versus enteroendocrine progenitors (Shroyer, et al., 2005). Mucus-secreting goblet cells migrate toward the villi tip, whereas antimicrobial peptide-secreting Paneth cells move to the base of the crypts. In addition, Paneth cells provide a niche for leucine-rich repeat–containing G-protein-coupled receptor 5 (Lgr5)-expressing stem cells in crypts (Sato, et al., 2011).

In mice, morphogenesis of the intestinal epithelium begins around embryonic day 14 (E14), followed by the reshaping of the endodermal pseudostratified epithelium to organize the villi and intervillous region (Grosse, et al., 2011). Villi begin to form from E15. At the beginning of intestinal development, proliferating progenitors that express ISC markers are ubiquitously distributed throughout the epithelium. In villi form, the villus cluster emits bone morphogenetic protein (BMP) signals, acting opposite to Wnt signaling; hence, putative ISCs are restricted to the villi base (Shyer, et al., 2015). In contrast, crypts begin to form approximately on postnatal day 7 (P7). Paneth cell–specific mRNAs, including cryptdin-4, cryptdin-5, lysozyme, matrilysin, and defensin-related sequences, have been detected in P1 mouse intestine (Darmoul, et al., 1997). Within 14 days of postnatal development, Paneth cells mature and express cryptdin proteins as a specific marker (Bry, et al., 1994, Inoue, et al., 2008). *Lgr5* deficiency leads

to premature Paneth cell differentiation in the small intestine without detectable effects on the differentiation of other cell lineages, or on proliferation or migration (Garcia, et al., 2009). However, the relation between the localization of Paneth cells at the bottom of the crypt and their maturation remains to be elucidated.

Our previous study showed that the absorptive cells of the jejunum and ileum change rapidly and dramatically from suckling to adult type during the weaning period (Fujita, et al., 2007). It has been suggested that the intestinal transcription factor Blimp-1 is a critical driver of the postnatal epithelial phenotype, whose expression loss in the third postnatal week is a likely requirement for the maturation of the neonatal epithelium to adult epithelium (Harper, et al., 2011, Muncan, et al., 2011). Organoid culture studies revealed that suckling–weaning transition is intrinsically programmed (Navis, et al., 2019). However, the factors driving Blimp-1 expression and loss remain unknown. Several epigenetic regulation events, including DNA methylation and histone modifications, are known to occur during early embryonic development. In chick embryos and neonates, it has been shown that spatiotemporal-specific epigenetic alterations could be critical for the late development of the liver, jejunum, and breast skeletal muscles (Li, et al., 2015). In contrast, abrupt changes in gene expression frequently occur in differentiating cells. These changes are accompanied by major chromatin structural changes that are triggered by modifications of the histone tail, such as acetylation, methylation, and phosphorylation (Rice, et al., 2003, Schubeler, et al., 2004). Among several histone modifications that have been identified, acetylation and methylation of histone H3 are extensively studied; regulation of H3 modifications is related to ON/OFF switching in transcription. In the small intestine, induction of sucrase-isomaltase (SI) gene expression during epithelial cell translocation from the crypt to the villi is associated with changes in histone H3 modifications from methylation at lysine 9 to di-acetylation at lysine 9 and 14 residues, as well as increased binding of Cdx-2 to the SI promoter region (Suzuki, et al., 2008). However, the epigenetic reprogramming event in IECs during neonatal–weaning transition is unknown.

In this study, we investigated the temporal histological changes in the ileum and the effect of methyltransferase inhibitors on epithelial development using organoid culture to elucidate the relationship between Paneth cell maturation and crypt formation.

Materials And Methods

Animals

Adult C57BL/6J mice (CLEA Japan) were used in this study. They were housed under conventional laboratory conditions at a constant temperature of 22 °C, with a 12 h light/dark cycle. Data for postnatal studies were assessed at postnatal days P0, P7, P14, P21 and P28. Animals were anesthetized by intraperitoneal injection of a mixture of medetomidine, midazolam, and butorphanol, followed by dissecting intact ileal tissues. The research protocol was approved by the Ethics Committee of the University of Occupational and Environmental Health and was conducted in accordance with the provisions of the Declaration of Helsinki, 1995 (as revised in Edinburgh, 2000).

Immunohistochemistry for tissue and organoids

For light microscopy, tissues and organoids were fixed for 16 h in 10% neutral buffered formalin at 4 °C. The tissues were embedded in paraffin and cut into 5-μm-thick sections. Sections were stained with hematoxylin and eosin (H&E) or subjected to immunohistochemistry. Organoids were embedded in Tissue-Tek® O.C.T. Compound (Sakura Finetek), frozen at −20 °C, and cut into 10-μm-thick sections. For immunohistochemistry, paraffin sections were prepared by boiling in 10 mM citrate buffer pH 6.0 for 15 min. After blocking with 1% bovine serum albumin, sections were incubated for 16 h at 4 °C with the following primary antibodies: anti-lysozyme C (1:200, goat polyclonal, Santa Cruz Biotechnology); anti-proliferating cell nuclear antigen (PCNA, 1:100, mouse monoclonal, Dako); anti-5-mC (1:300, rabbit monoclonal, Cell Signaling Technology); and anti-H3K4, 9, 27, 36, and 79me3 (1:300, rabbit monoclonal, Cell Signaling Technology). Before incubation with secondary antibodies, the tissues were washed to remove the unbound antibodies. The sections were then incubated with secondary antibodies (1:1000 dilution; Alexa Fluor 488 and/or Alexa Fluor 555, Invitrogen) for 1 h at 25 °C and mounted using UltraCruz™ Mounting Medium with DAPI (Santa Cruz Biotechnology). The samples were observed under a fluorescence microscope (Axioskop 2 plus or Apotome. 2, Carl Zeiss).

Electron microscopy

For electron microscopy, tissues and organoids were fixed for 16 h in 2.0% paraformaldehyde and 2.5% glutaraldehyde in 0.1 M phosphate buffer (PB) at 4 °C, and post-fixed in 1% osmium tetroxide in 0.1 M PB for 2 h at 4 °C. The specimens were dehydrated and embedded in an epoxy resin. Semi-thin sections were stained with toluidine blue O (Sigma-Aldrich) and observed under a light microscope (Axioskop 2 plus). Thin sections were stained with uranyl acetate and lead citrate and observed under a transmission electron microscope (TEM) at 80 kV (1400Plus, JEOL).

Organoid culture

Intestinal organoids were cultured according to the Sugimoto and Sato protocol (Sugimoto and Sato, 2017). The terminal ileum was harvested from C57BL/6J mice at P4, P7, and P10, and the tissues were sliced into segments. The crypts were isolated by 2.5 mM ethylenediaminetetraacetic acid (EDTA) in PBS for 30 min at 4 °C and pelleted by centrifugation at 400 × *g* for 3 min at 4 °C. The crypts were then resuspended in Matrigel (Corning) and transferred to 48-well plates. After polymerization, mouse IntestiCult organoid growth medium (Stem Cell Technologies) supplemented with penicillin-streptomycin (100 U/mL) was added to each well and incubated at 37 °C. 3 days after crypt isolation, 0.2 μM 3-Deazaneplanocin A hydrochloride (DZNep, Abcam) or 20 μM GSK126 (Bio Vision) was added to the medium to inhibit the activity of histone methyltransferase EZH2, which mediates H3K27 methylation. After 3 days of incubation with the EZH2 inhibitor, the organoids were observed under a light microscope.

Statistical analysis

Results are expressed as the mean ± standard error of the mean (SEM). Statistical differences were assessed using Dunnett's test. Statistical significance was set at $p < 0.05$.

Results

Morphological changes in the ileum during neonatal–weaning transition

It remains unclear whether crypt formation is related to Paneth cell maturation. To test this, we histologically observed the mouse ileum from neonatal to adult stages in mice (Fig. 1a–f). Villi were present in the P0 ileum, and a time-dependent increase in length and width was observed. Between the villi, shallow crypts were present at P14 (Fig. 1c), and a time-dependent increase in depth was observed (Fig. 1c–f). Goblet cells were dispersed in IECs from crypts to villi. The supranuclear lysosomes of absorptive cells were enlarged in P7 and P14 (Fig. 1b, c). However, there were no large lysosomes in the absorptive cells of P21 mice. Paneth cells, including eosinophilic granules, were observed at the bottom of the shallow crypts of P14 ileum (Fig. 1c). The number of Paneth cells and granules within the cell increased in a time-dependent manner (Fig. 1d–f).

For detailed structural analysis of IECs, we next observed the ileum under a TEM (Fig. 2a–f). In P0 mice, absorptive cells, goblet cells, enteroendocrine cells, undifferentiated cells, and dividing cells were observed (Fig. 2a). In addition to typical goblet cells (Fig. 2d), some goblet cells containing secretory granules with a small dense core, called granular goblet cells, were observed (Fig. 2e). No typical Paneth cells were observed in the epithelium. Cell types lining the P7 epithelium were similar to those in the P0 epithelium. In addition to P0 granular goblet cells, another type of granular goblet cell was observed in the primordia of the crypt (Fig. 2b, f). The cells had a core that was larger than the first type, and varied in size in the secretory granules. Many dense core secretory granules enriched with a clear halo were observed in Paneth cells positioned at the bottom of the P14 crypts (Fig. 2c). Subsequently, the number of Paneth cells increased.

Epigenetic modification in the ileum during neonatal–weaning transition

To examine the epigenetic event, we attempted to detect 5-methylcytosine (5-mC) for DNA methylation and H3K4, 9, 27, 36, and 79me3 for histone modifications in the epithelium of the developing ileum. There was no significant alteration in the expression of 5-mC, H3K4, 9, 36, or 79me3 in the IECs of the intervillous region or crypts from neonatal to weaning mice (data not shown). However, IECs located at the base of the crypt were positive for H3K27me3 after P14 (Fig. 3a–d). H3K27me3-positive cells in the crypts were negative for PCNA (Fig. 3e–h) and positive for lysozyme C (Fig. 4a–d).

Effect of the EZH2 inhibitor on ileal organoid culture

To examine the effect of H3K27 trimethylation on the development of the ileal epithelium, we used two types of EZH2 inhibitors, DZNep and GSK126, to inhibit the histone methyltransferase EZH2, which mediates the trimethylation of H3K27. The ileal crypts were isolated from the ileum of P4, P7 or P10 mice and cultured as organoids. DZNep or GSK126 was added to the culture medium after 3 days of culture. Subsequently, we observed the organoids under a light microscope (Fig. 5). In the culture isolated from P4 and P7, the crypt budding was inhibited, and organoids appeared in spheroid form in the DZNep- and GSK126-treated groups as compared to that in control group (Fig. 6a–c). H3K27me3 positive cells were observed in organoids of the control group, but not in those of DZNep- and GSK126-treated groups (Fig. 6d–f). However, regardless of EZH2 inhibition, new crypt budding occurred in most organoids isolated from P10 mouse ileum, although the depth and number of crypts in DZNep- and GSK126-treated organoids were less than control group (Fig. 7). In the organoids isolated from P7 mouse ileum, there were Paneth cells in addition to goblet cells and two types of granular goblet cells (Fig. 8a). However, Paneth cells were rarely observed in the DZNep- and GSK126-treated groups, although goblet cells and two types of granular goblet cells were observed (Fig.8b, c). In the organoids derived from P10 mouse ileum (Fig.8d-f), mature Paneth cells were observed regardless of EZH2 inhibition, although the cell number in EZH2 inhibited organoids was smaller than in the control group. Some absorptive cells had an endocytic membrane system including invaginations between microvilli, vesicles, tubules, endosomes, as seen in the suckling ileum, in the DZNep- and GSK126-treated groups (Supplementary Fig. 1).

Discussion

In this study, the second type of granular goblet cells with secretory granules enclosed a larger and irregular dense core appeared in the ileal epithelium, later than the first granular goblet cells, and earlier than Paneth cells. The cells were located in the ileal crypt, deeper than the first granular goblet cells, and shallower than Paneth cells.

Granular goblet cells in the upper part of the crypts, which we call the first type, differ from other goblet cells because of the presence of small dense granules embedded within the mucus globules (Calvert, et al., 1988, Cheng, 1974a). In addition, the presence of intermediate cells between Paneth and goblet cells has been reported in normal mice (Cheng, 1974b, Troughton and Trier, 1969) and humans (Subbuswamy, 1973). Furthermore, the appearance of intermediate cells has recently been reported in various knockout mice (Jackson, et al., 2020, Khaloian, et al., 2020, Watanabe, et al., 2016), ileitis (Jackson, et al., 2020) and inflammatory bowel disease (IBD) (Khaloian, et al., 2020).

Previously, intermediate cells were considered immature Paneth cells or young goblet cells in the small intestine (Troughton and Trier, 1969) or independent of the presence of the Paneth cells (Calvert, et al., 1988). However, the cellular differentiation between Paneth and goblet cells is considered to probably occur via intermediate cells (Mantani, et al., 2014). In our study, the first granular goblet cells appeared in the epithelium of the villi and intervillous region. Second granular goblet cells that were similar to

intermediate cells appeared below the first granular goblet cells. Moreover, Paneth cells appeared at the bottom of the crypt after P14. The appearance of these three cell types differs temporally and spatially. In addition, we observed another cell type that had a few coreless granules (data not shown). Recently, a study revealed that the phenotype of intermediate cells is consistent with an immature Paneth cell (Dekaney, et al., 2019). Our findings indicate that two types of granular goblet cells, especially in the second type, are precursors of Paneth cells; however, further research is needed on the expression of specific marker genes and proteins.

In the present study, Paneth cells located at the bottom of the crypt in P14 mice ilea had trimethylated histone H3 lysine 27. Inhibition of EZH2 in organoid culture suppressed stage-specific crypt budding. Post-transcriptional modification of histones plays an essential role in the regulation of chromatin structure and gene transcription. Histone methylation occurs in histone H3 at lysine 4, 9, 14, 27, 36 and 79 residues, and in histone H4 at lysine 20 and 59 residues. Generally, H3 methylation at lysine 4, 36, and 79 is correlated with euchromatin and transcriptional activation, whereas H3 methylation at lysine 9 and 27, and H4 at lysine 20 is associated with heterochromatin and transcriptional repression. However, post-transcriptional modification of histones fluctuates with the developmental stage (Lee, et al., 2005). The reduction or suppression of histone H3K27 trimethylation is also related to intestinal tumorigenesis and cancer (McCleland, et al., 2015).

Enhancer of zeste homolog 2 (EZH2), as part of the polycomb repressive complex 2 (PRC2), selectively catalyzes H3 lysine 27 trimethylation. In the murine jejunum and ileum, EZH2 and suppressor of Zeste-12 (SUZ12) were expressed in non-differentiated proliferative crypt IECs, and the PRC2 complex ensures the proper response of IECs to cell density (Turgeon, et al., 2013). PRC2 regulates intestinal homeostasis, maintaining progenitor cell proliferation and an optimal balance between secretory and absorptive lineage differentiation programs (Chiacchiera, et al., 2016, Koppens, et al., 2016). PRC2 activity is required to maintain cell plasticity at the bottom of the intestinal crypt and the repression of Atoh1 and Gfi1, which are master regulators of goblet cells (Chiacchiera, et al, 2016). However, cell-specific trimethylation at H3K27 has not been reported in the developing small intestine.

In this study, H3K27 trimethylation was detected in Paneth cells at the bottom of the crypts during the second week of postnatal mice. Organoid culture from early in the second postnatal week mouse was suppressed crypt budding and Paneth cell maturation by the EZH2 inhibitor, unlike late in the second week. These results suggest that H3K27 trimethylation in Paneth cells at the bottom of the crypts began early in the second postnatal week and was almost complete during the second week, and it was related to its functional and morphological maturation. In our observation, the transition of the absorptive cell from sucking to weaning was assumed to be completed after Paneth cell maturation. Paneth cell maturation, which is involved not only in the secretion of antimicrobial peptides but also in the construction of the ISC niche, is related to the formation of the crypt and its localization. However, crypts have been reported to form independently of Paneth cells in mice lacking lysine-specific demethylase 1A (Zwiggelaar, et al., 2020). Consistent with our observations, organoids derived from fetal IECs undergo suckling–weaning transition, and organoids with crypts gradually increase, contrary to decreasing

spheroids (Navis, et al., 2019). However, the authors of that paper concluded that spheroids transition to organoids and do not reflect the maturation stages. Further research is needed to determine whether all cell types mature or not. The intestinal transcription factor Blimp-1, which is selectively expressed in mouse IECs during embryonic and postnatal development, lost its expression during suckling–weaning transition (Muncan et al., 2011). Although it was assumed that H3 trimethylation at lysine 27 participates in suppression of Blimp-1, the gene expression that is suppressed by H3K27 trimethylation remains unknown. To address this, understanding the mechanism by which intermediate cells that are regarded as premature Paneth cells, appearing aberrantly in intestinal diseases such as IBD, is required.

In conclusion, our data show that post-transcriptional modification of histones, particularly H3 at lysine 27 trimethylation, exerted structural and functional maturation of Paneth cells during postnatal development in mice.

Declarations

Acknowledgements

We would like to thank Editage (www.editage.com) for English language editing.

Author contributions

RB and HM designed the research; RB, KK and KN performed the research; RB wrote the draft paper; HM and MF edited the final manuscript. All authors reviewed the manuscript.

Funding

This work was supported by JSPS KAKENHI Grant Numbers: 17K00903 (RB), 16K00934 (MF), and 21K07927 (HM).

Conflict of interest

The authors of this article declare no conflicts of interest.

Data availability

The datasets generated during and/or analysed during the current study are available from the corresponding author on reasonable request.

References

1. Barker N, Clevers H (2007) Tracking down the stem cells of the intestine: strategies to identify adult stem cells. Gastroenterology 133:1755-1760
2. Bry L, Falk P, Huttner K, Ouellette A, Midtvedt T, Gordon JI (1994) Paneth cell differentiation in the developing intestine of normal and transgenic mice. Proc Natl Acad Sci U S A 91:10335-10339
3. Calvert R, Bordeleau G, Grondin G, Vezina A, Ferrari J (1988) On the presence of intermediate cells in the small intestine. Anat Rec 220:291-295
4. Cheng H (1974a) Origin, differentiation and renewal of the four main epithelial cell types in the mouse small intestine. II. Mucous cells. Am J Anat 141:481-501
5. Cheng H (1974b) Origin, differentiation and renewal of the four main epithelial cell types in the mouse small intestine. IV. Paneth cells. Am J Anat 141:521-535
6. Chiacchiera F, Rossi A, Jammula S, Zanotti M, Pasini D (2016) PRC2 preserves intestinal progenitors and restricts secretory lineage commitment. EMBO J 35:2301-2314
7. Darmoul D, Brown D, Selsted ME, Ouellette AJ (1997) Cryptdin gene expression in developing mouse small intestine. Am J Physiol 272:G197-206
8. Dekaney CM, King S, Sheahan B, Cortes JE (2019) Mist1 Expression Is Required for Paneth Cell Maturation. Cell Mol Gastroenterol Hepatol 8:549-560
9. Fre S, Huyghe M, Mourikis P, Robine S, Louvard D, Artavanis-Tsakonas S (2005) Notch signals control the fate of immature progenitor cells in the intestine. Nature 435:964-968
10. Fujita M, Baba R, Shimamoto M, Sakuma Y, Fujimoto S (2007) Molecular morphology of the digestive tract; macromolecules and food allergens are transferred intact across the intestinal absorptive cells during the neonatal-suckling period. Med Mol Morphol 40:1-7
11. Garcia MI, Ghiani M, Lefort A, Libert F, Strollo S, Vassart G (2009) LGR5 deficiency deregulates Wnt signaling and leads to precocious Paneth cell differentiation in the fetal intestine. Dev Biol 331:58-67
12. Grosse AS, Pressprich MF, Curley LB, Hamilton KL, Margolis B, Hildebrand JD, Gumucio DL (2011) Cell dynamics in fetal intestinal epithelium: implications for intestinal growth and morphogenesis. Development 138:4423-4432
13. Harper J, Mould A, Andrews RM, Bikoff EK, Robertson EJ (2011) The transcriptional repressor Blimp1/Prdm1 regulates postnatal reprogramming of intestinal enterocytes. Proc Natl Acad Sci U S A 108:10585-10590
14. Inoue R, Tsuruta T, Nojima I, Nakayama K, Tsukahara T, Yajima T (2008) Postnatal changes in the expression of genes for cryptdins 1-6 and the role of luminal bacteria in cryptdin gene expression in mouse small intestine. FEMS Immunol Med Microbiol 52:407-416
15. Jackson DN, Panopoulos M, Neumann WL, Turner K, Cantarel BL, Thompson-Snipes L, Dassopoulos T, Feagins LA, Souza RF, Mills JC, Blumberg RS, Venuprasad K, Thompson WE, Theiss AL (2020) Mitochondrial dysfunction during loss of prohibitin 1 triggers Paneth cell defects and ileitis. Gut 69:1928-1938

16. Khaloian S, Rath E, Hammoudi N, Gleisinger E, Blutke A, Giesbertz P, Berger E, Metwaly A, Waldschmitt N, Allez M, Haller D (2020) Mitochondrial impairment drives intestinal stem cell transition into dysfunctional Paneth cells predicting Crohn's disease recurrence. Gut 69:1939-1951
17. Koppens MA, Bounova G, Gargiulo G, Tanger E, Janssen H, Cornelissen-Steijger P, Blom M, Song JY, Wessels LF, van Lohuizen M (2016) Deletion of Polycomb Repressive Complex 2 From Mouse Intestine Causes Loss of Stem Cells. Gastroenterology 151:684-697 e612
18. Lee DY, Teyssier C, Strahl BD, Stallcup MR (2005) Role of protein methylation in regulation of transcription. Endocr Rev 26:147-170
19. Li C, Guo S, Zhang M, Gao J, Guo Y (2015) DNA methylation and histone modification patterns during the late embryonic and early postnatal development of chickens. Poult Sci 94:706-721
20. Mantani Y, Nishida M, Yuasa H, Yamamoto K, Takahara E, Omotehara T, Udayanga KG, Kawano J, Yokoyama T, Hoshi N, Kitagawa H (2014) Ultrastructural and histochemical study on the Paneth cells in the rat ascending colon. Anat Rec (Hoboken) 297:1462-1471
21. McCleland ML, Soukup TM, Liu SD, Esensten JH, de Sousa e Melo F, Yaylaoglu M, Warming S, Roose-Girma M, Firestein R (2015) Cdk8 deletion in the Apc(Min) murine tumour model represses EZH2 activity and accelerates tumourigenesis. J Pathol 237:508-519
22. Muncan V, Heijmans J, Krasinski SD, Büller NV, Wildenberg ME, Meisner S, Radonjic M, Stapleton KA, Lamers WH, Biemond I, van den Bergh Weerman MA, O'Carroll D, Hardwick JC, Hommes DW, van den Brink GR (2011) Blimp1 regulates the transition of neonatal to adult intestinal epithelium. Nat Commun 2:452
23. Navis M, Martins Garcia T, Renes IB, Vermeulen JL, Meisner S, Wildenberg ME, van den Brink GR, van Elburg RM, Muncan V (2019) Mouse fetal intestinal organoids: new model to study epithelial maturation from suckling to weaning. EMBO Rep 20:
24. Rice JC, Briggs SD, Ueberheide B, Barber CM, Shabanowitz J, Hunt DF, Shinkai Y, Allis CD (2003) Histone methyltransferases direct different degrees of methylation to define distinct chromatin domains. Mol Cell 12:1591-1598
25. Sato T, van Es JH, Snippert HJ, Stange DE, Vries RG, van den Born M, Barker N, Shroyer NF, van de Wetering M, Clevers H (2011) Paneth cells constitute the niche for Lgr5 stem cells in intestinal crypts. Nature 469:415-418
26. Schubeler D, MacAlpine DM, Scalzo D, Wirbelauer C, Kooperberg C, van Leeuwen F, Gottschling DE, O'Neill LP, Turner BM, Delrow J, Bell SP, Groudine M (2004) The histone modification pattern of active genes revealed through genome-wide chromatin analysis of a higher eukaryote. Genes Dev 18:1263-1271
27. Shroyer NF, Wallis D, Venken KJ, Bellen HJ, Zoghbi HY (2005) Gfi1 functions downstream of Math1 to control intestinal secretory cell subtype allocation and differentiation. Genes Dev 19:2412-2417
28. Shyer AE, Huycke TR, Lee C, Mahadevan L, Tabin CJ (2015) Bending gradients: how the intestinal stem cell gets its home. Cell 161:569-580
29. Subbuswamy SG (1973) Paneth cells and goblet cells. J Pathol 111:181-189

30. Sugimoto S, Sato T (2017) Establishment of 3D Intestinal Organoid Cultures from Intestinal Stem Cells. Methods Mol Biol 1612:97-105
31. Suzuki T, Mochizuki K, Goda T (2008) Histone H3 modifications and Cdx-2 binding to the sucrase-isomaltase (SI) gene is involved in induction of the gene in the transition from the crypt to villus in the small intestine of rats. Biochem Biophys Res Commun 369:788-793
32. Troughton WD, Trier JS (1969) Paneth and goblet cell renewal in mouse duodenal crypts. J Cell Biol 41:251-268
33. Turgeon N, Blais M, Delabre JF, Asselin C (2013) The histone H3K27 methylation mark regulates intestinal epithelial cell density-dependent proliferation and the inflammatory response. J Cell Biochem 114:1203-1215
34. Watanabe N, Mashima H, Miura K, Goto T, Yoshida M, Goto A, Ohnishi H (2016) Requirement of Galphaq/Galpha11 Signaling in the Preservation of Mouse Intestinal Epithelial Homeostasis. Cell Mol Gastroenterol Hepatol 2:767-782 e766
35. Zwiggelaar RT, Lindholm HT, Fosslie M, Terndrup Pedersen M, Ohta Y, Diez-Sanchez A, Martin-Alonso M, Ostrop J, Matano M, Parmar N, Kvaloy E, Spanjers RR, Nazmi K, Rye M, Drablos F, Arrowsmith C, Arne Dahl J, Jensen KB, Sato T, Oudhoff MJ (2020) LSD1 represses a neonatal/reparative gene program in adult intestinal epithelium. Sci Adv 6:

Figures

Figure 1

Histological changes in the mouse ileum from neonatal to adult stages. Morphological analysis was performed on 5-µm-thick paraffin-embedded sections stained with H&E. **a** P0, **b** P7, **c** P14, **d** P21, **e**. P28, **f**. adult. Paneth cells, including eosinophilic granules (arrowhead), were observed at the bottom of the ileal crypts after P14. Bar 20 µm

Figure 2

Ultrastructure of mouse ileal epithelial cells from neonatal to suckling stages. Ultrastructural analysis of IECs in the intervillous region or crypts was performed using a TEM. **a** P0, **b** P7, **c** P14, **d** typical goblet cell, **e** first granular goblet cell, **f** second granular goblet cell. First granular goblet cells (white arrowhead) and second granular goblet cells (white arrow) were observed before the appearance of Paneth cells (black arrowhead). Bars 2 µm

Figure 3

Immunohistochemical analysis of epigenetic modification in the mouse ileum from neonatal to weaning stages. Immunohistochemistry was performed on 5-μm-thick paraffin-embedded sections of the mouse ileum. **a, e** P0, **b, f** P7, **c, g** P14, **d, h** P21. **a–d** Anti-H3K27me3 antibody was used. Bar 20 μm. **e–h** Anti-H3K27me3 and anti-PCNA antibodies were used. Bar 10 μm. IECs located at the bottom of the crypt were positive for H3K27me3 (green, arrowhead) which were negative for PCNA (magenta) after P14. The red channel was replaced with the magenta channel to improve visualization.

Figure 4

Immunohistochemical analysis of trimethylated H3K27 in the mouse ileum from neonatal to weaning stages. Immunohistochemistry was performed on 5-μm-thick paraffin-embedded sections of the mouse ileum. **a** P0, **b** P7, **c** P14, **d** P21. Antibodies anti-H3K27me3 and anti-lysozyme C, and DAPI (blue) were used. IECs located at the bottom of the crypt were positive for H3K27me3 (green, arrowhead) and positive for lysozyme C (magenta) after P14. The red channel was replaced with the magenta channel to improve visualization. Bars 10 μm

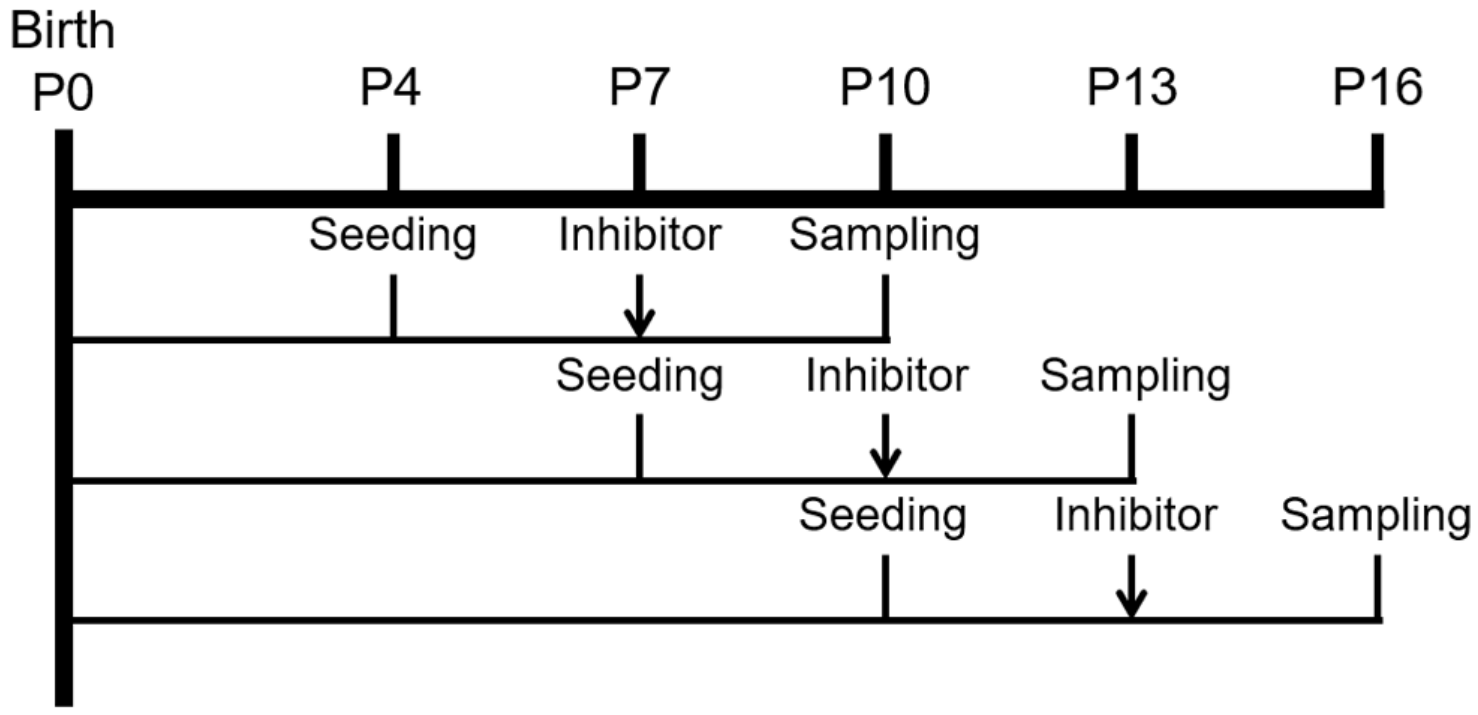

Figure 5

Scheme of ileal organoid culture. Organoids isolated from P4, P7, and P10 mouse ilea were cultured for 3 days. After an additional 3 days of culture under EZH2 inhibition, the samples were collected.

Figure 6

Inhibition of H3K27 trimethylation in the ileal organoid culture. The inhibitory effect was demonstrated using organoid culture of the ileal crypt. Organoids isolated from P7 mouse ileum were observed under a light microscope (**a–c**). Bar 500 μm. The DZNep- (**b**) and GSK126- (c) treated groups inhibited crypt growth (black arrowhead) compared to the control group **(a**). Immunocytochemistry using anti-H3K27me3 antibody was applied to each group (**d–f**). Bar 50 μm. H3K27me3-positive cells (white arrowhead) were observed in organoids of the control group (**d**), but not in those of DZNep- and GSK126-treated groups (**e**, **f**).

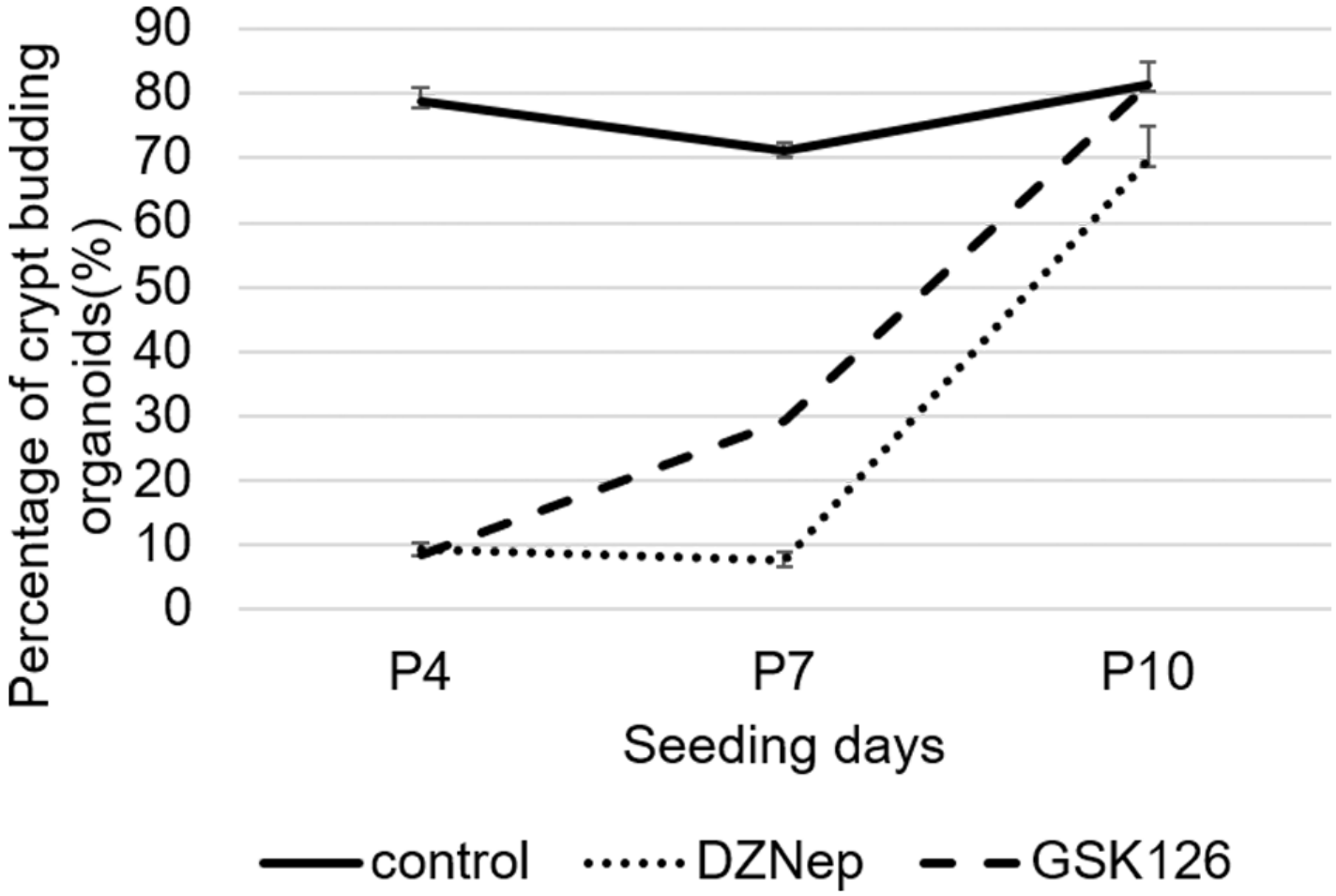

Figure 7

Percentage of crypt budding organoids (n = 3 wells from a single organoid culture). Crypt budding was inhibited in the DZNep- and GSK126-treated groups as compared to that in control group isolated from P4 and P7 mouse ileum. Crypt budding occurred in most organoids isolated from P10 mouse ileum, regardless of EZH2 inhibition.

Figure 8

Inhibition of H3K27 trimethylation of Paneth cells in ileal organoid culture. Paneth cells in organoids isolated from P7 (**a–c**) and P10 (**d–f**) mouse ileum were observed under a TEM. Bar 1 μm. In the control group derived from the P7 ileum, goblet cells, two types of granular goblet cells and Paneth cells **(a**) were observed. Paneth cells had dense core secretory granules with a halo (arrowheads). In the groups treated with DZNep (**b**) and GSK126 (**c**), goblet cells and two types of granular goblet cells were observed. The secretory granules of the second granular goblet cells had a smaller dense core (white arrows) than Paneth cells. However, little or no Paneth cells were observed. In the organoids from P10 ileum (**d–f**), goblet cells, two types of granular goblet cells and Paneth cells were observed. Paneth cells had dense core secretory granules with a halo (arrowheads).

Supplementary Files

This is a list of supplementary files associated with this preprint. Click to download.

- SupplementaryFigure.1.tif